

# Determining the orientation of the Magnetic Fields of Molecular Clouds based on Polarized Dust Emission Observations

Alison Andrade,<sup>1</sup>

<sup>1</sup>*Queen's University*

4 April 2023

## ABSTRACT

This paper will examine polarimetric observations of the Vela C and Orion A molecular clouds, to gain insight into the 3D structure of their magnetic fields. As molecular clouds have complex structures, factors such as column density, grain alignment efficiency, temperature, and dispersion in the polarization angle must be considered when analyzing the results. An analysis of Vela C is made using the polarization fraction, ( $p$ ), and the dispersion in the polarization angle, ( $S$ ), to examine the inclination angle of the cloud's magnetic field with respect to the plane-of-sky. Additionally, the magnetic field inclination angle will be estimated in four regions of Vela C, based on the varying polarization fraction in each region. In Orion A, previous observations have been made using Faraday rotation to gain insight into the 3D structure of the field in the cloud. Polarimetric observations will be used on Orion A to determine whether the polarization is consistent with these observations. The analysis also shows that regions with higher column density,  $N_H$ , tend to have lower polarization fractions, likely due to the reduced efficiency of grain alignment in denser regions. These factors can affect the polarization in the clouds and, therefore, must be taken into consideration when determining the orientation of the magnetic field in these regions. The results show that Vela C has an overall high inclination angle, ranging from 55.5°–66.5° with respect to plane-of-sky, and that the orientation of the field increases towards the south regions of the cloud. The polarization analysis of Orion A showed an increase in the polarization fraction around the main filamentary structure in the cloud, which would indicate a magnetic field inclination angle closer to the plane-of-sky around the cloud.

**Key words:** polarization – magnetic fields – molecular clouds – column density

## 1 INTRODUCTION

Magnetic fields in molecular clouds are crucial to the formation and evolution of stars, yet they can be challenging to observe and their properties are not well known. Dust and gas in the cloud can accrete along magnetic field lines, and this can inhibit the collapse of the cloud to form stars. Thus, magnetic fields can be a potential factor in inhibiting star formation. By understanding the structure of magnetic fields in these regions, we can gain a better understanding of the structure of molecular clouds, and the formation of stars.

Several methods are being used to determine 3D structure of magnetic fields in molecular clouds. Observations such as the strength, direction, and orientation of the magnetic field can be determined using various line-of-sight (LOS) and plane-of-sky (POS) observations. The magnetic field of both line-of-sight,  $B_{LOS}$ , and plane-of-sky,  $B_{POS}$ , are required to infer the 3D structure of the fields. This paper will use dust emission polarization to analyse properties of two molecular clouds, Vela C and Orion A, with the goal of determining the orientation of their magnetic fields and their 3D structures.

Linearly polarized dust emission can be used to create large-scale maps to study the inclination angles of magnetic fields in molecular clouds. It is a commonly used method as it is relatively inexpensive yet efficient, and can be used to trace over large areas and a wide range of densities. Molecular clouds are composed of small, non-spherical

dust grains whose minor axes will orient parallel to the magnetic field of the cloud. Current data suggests that the primary cause of this alignment is due to radiative torques (RATs) that are caused by anisotropic radiation fields (Fissel et al. (2016)). This orientation will result in the light emitted from the cloud being polarized, which in turn implies the presence of a magnetic field. The nature of this method relies heavily on the orientation of the dust grains, and as a result, external factors that can influence the alignment of grains will be taken into consideration, such as the column density, grain alignment efficiency and temperature. The orientation of these magnetic fields can then be deduced using polarized dust emission maps (Pattle et al. (2022)).

The magnetic field orientation within a molecular cloud can be mapped on the plane-of-sky by measuring the linear polarization emitted by dust grains within the cloud. Rotating the polarization orientation by 90 degrees, can determine the average  $B_{POS}$ , and can be sensitive to regions of high dust and low grain alignment (Sullivan et al. (2021)).

As molecular clouds are large, complex structures, their physical properties will change in different regions of the cloud, and this must be taken into consideration when analysing these observations. One of the main properties that will affect the polarization in the cloud is the column density. In regions of high column density the grains will be better shielded from short wavelength light, which is

expected to be responsible for aligning the dust grains with respect to the magnetic field. As a result, the polarization fraction can decrease in regions of high column density. A high orientation of the magnetic field with respect to the plane-of-sky can also contribute to depolarization in observations. Additionally, if there are substantial variations in the orientation of the magnetic field within a particular region, it may result in depolarization due to a significant degree of cancellation. Other factors that can play a smaller role in depolarization are the temperature, jet outflow/feedback, gravity and other external forces (Pattle et al. (2022)).

There are several polarization parameters that can be used to infer the  $B_{POS}$ . The polarization fraction,  $p$ , is the fraction of light that is linearly polarized as a result of the field in the clouds. This parameter is sensitive to the grain alignment efficiency with respect to the magnetic field. As a result, an additional parameter that accounts for the dispersion in the polarization angle must be considered, the  $S$ -dispersion. A more accurate measurement of the orientation of the magnetic field can be made in regions where the dispersion is lower (Chen et al. (2019)). In addition, the hydrogen column density,  $N_H$ , is also taken into consideration, to look for the effects of depolarization due to loss of grain alignment efficiency, rather than inclination angle changes. The column density can affect the alignment of grains, and this can in turn affect the amount of polarized light that is emitted from the cloud.

In Vela C, the overall inclination angle will be estimated from  $p$ , described in section 3, and will closely follow the approach as described in Chen et al. (2019). Vela C will be broken up into four regions based on its temperature and column density properties, and the inclination angles of each of these regions will be measured. The dispersion in the polarization angles,  $S$ , will also be accounted for in calculating the inclination angles of each region. These observations can be compared with observations from Chen et al. (2019), where similar calculations were performed from synthetic observations to determine the inclination angle of the whole cloud.

The analysis of the Orion A molecular cloud involves studying the polarization fraction and column density, to understand how they vary throughout the cloud. Previous findings by Tahani (2022) using Faraday rotation showed a reversal in the magnetic field throughout the cloud. The polarization observations will be analysed to determine if they are consistent with these findings. In a similar manner to Vela C, Orion A will also be divided up into regions based on its column density. Variations in these findings can be attributed to the structure of the cloud, and other properties that affect the polarization fraction, i.e., grain alignment efficiency, inclination angle of the magnetic field and column density. Overall, the analysis of Orion A will provide insights into the understanding of the structure of its magnetic field, and determine the accuracy of using the polarization to achieve these results.

## 2 THE STRUCTURE OF MOLECULAR CLOUDS

### 2.1 Filaments and substructures

Molecular clouds are complex in structure and can vary in temperature and column density, depending on different subregions of the cloud. Most stars form in Giant Molecular Clouds(GMCs) where  $M_{cloud} > 10^5 M_\odot$  (Chen et al. (2019)). Filamentary structures in the clouds are defined as regions of higher column density, that can be divided based on the  $A_V$  magnitude and multi-resolution analysis(MRA) of the column density and temperature (Hill et al. (2011)). 70% of prestellar cores are found in the densest filaments, where column densities exceed  $\sim 7 \times 10^{21} \text{ cm}^{-2}$  (Pattle et al. (2022)). Magnetic

fields play a significant role in the formation of filamentary structures in clouds, which gives insight into their role in the formation of stars.

### 2.2 Magnetic field structure in molecular clouds

If magnetic fields are well coupled to the gas, they can influence the formation of the clouds substructure. Factors that can affect the magnetic fields and structure in the clouds include the column density, temperature, turbulence, gravity and other environmental factors. Cloud simulations on the order of  $\sim 10$  pc show that molecular clouds that are strongly magnetized have an ordered magnetic field structure, whereas weaker-field simulations show a more disordered field structure Pattle et al. (2022). Large-scale dust polarization observations have shown that significant bends in  $B_{POS}$  can indicate that the magnetic field direction has been altered by other environmental factors in the cloud (Pattle et al. (2022); Planck Collaboration XIX (2015)). An example of this can be seen in regions of the Vela C molecular cloud (Figure 2), and will be further discussed in section 4.1.2.

Magnetic fields can also influence how filamentary structures are formed. Strong magnetic fields can create a more ordered flow of gas, as opposed to turbulent gas motions, and sets a preferential gas flow in the direction parallel to the field. This resists compression in the perpendicular direction, which can inhibit the clouds collapse. It is shown that dense filaments align preferentially in the direction perpendicular to the magnetic field, while lower density filaments align parallel to the magnetic field (Pattle et al. (2022)).

The following section will discuss correlations seen between the polarization fraction  $p$ , the column density  $N_H$ , the dispersion in polarization angle  $S$ , and the temperature  $T$ .

### 2.3 Correlations in $p$ , $N_H$ , $S$ and $T$

Prior analysis for the correlation between the polarization fraction,  $p$ , and the column density,  $N_H$ , shows that these two variables are anti-correlated (Planck Collaboration XIX (2015)). This relationship can be due to factors such as the de-polarization from changes in grain alignment efficiency in regions of high column density (Planck Collaboration XIX (2015); Sullivan et al. (2021)). For an increase in the column density,  $N_H$ , there are more dust grains that are shielded by other dust grains, which will result in the polarization from the dust column to be lower. The dust grain alignment efficiency also plays a big part in the correlation of  $p$  and  $N_H$ . Magnetohydrodynamic (MHD) simulations in King et al. (2017) showed that an increase in  $p$  for a decrease in  $N_H$  can be reproduced based on individual properties of the cloud. For example, in a polarimetric observation on Vela C, this correlation could not be initially produced when the model did not include a loss of grain alignment. By including a simple analytic model for the decrease in grain alignment efficiency with column density, it was possible to reproduce these trends in Vela C (Fissel et al. (2016)).

In contrast to these results, Sullivan et al. (2021) showed little correlation between the  $p$  and  $N_H$  parameters in 3 out of 9 surveyed clouds. Possible reasons for this discrepancy was likely due to the difference in the range of column densities taken by different studies. While Planck Collaboration XIX (2015) surveyed more diffuse regions, Sullivan et al. (2021) surveyed regions of column density within a certain, higher threshold, which would likely have lower grain alignment efficiency. Thus, this discrepancy would require further studies of various clouds of diverse properties, in order to fully understand this correlation. In section 4.2, different regions of Orion

A will be analysed based on the column density and orientation of the magnetic field, to determine variations in the polarization fraction caused by the column density.

Additionally, previous studies have noted a negative correlation between the polarization fraction and the dispersion in the polarization angle,  $\log(p)$  and  $\log(S)$  (Fissel et al. (2016); Planck Collaboration XIX (2015); Aghanim et al. (2020); Sullivan et al. (2021)). A higher dispersion in  $S$  can be a result of several factors in the cloud that can affect the polarization and the grain alignment. For a high inclination angle on the plane-of-sky, there is an increase in the  $S$ -dispersion. This is because the field appears more disordered when projected on the plane of the sky. In polarization observations, grains are assumed to be homogeneously aligned, and as a result, the inclination angle of the magnetic field becomes the dominant source of depolarization. Synthetic studies on Vela C have shown a higher negative slope in  $p$  vs  $S$  due to it's high inclination angle. Thus in analysing the inclination angle using  $p$ , a more accurate value can be determined by eliminating regions of high  $S$  dispersion (Chen et al. (2019)).

Finally, there is also a strong anti-correlation between the temperature,  $T$ , and  $N_H$  (Fissel et al. (2016)). As previously mentioned,  $p$  is anti-correlated with  $N_H$ , which suggests that an increase in  $T$  would lead to an increase in  $p$ . There are two possible explanations for the observed decrease in  $T$  for an increase in  $N_H$ . One possibility is that high column density (and therefore low temperature) dust columns have greater magnetic field disorder. This could be due to either higher field disorder at high particle densities, or high column density sightlines passing through more cloud material along the line-of-sight. The second explanation involves the RATs model of grain alignment, where anisotropic radiation fields are responsible for aligning dust grains with the local magnetic field. Grains near the surfaces of molecular clouds (low column density, high temperature) may show a higher average polarization fraction, while dust grain properties may change at high densities, such as becoming rounder due to accretion of icy mantles. As a result, an increase in  $T$  is correlated with an increase in  $p$ . While  $p$  will not be compared to temperature maps in this study, it is important to consider it as a variable when looking at the changing polarization in different regions of the cloud.

## 2.4 Sources of depolarization

Several factors can lead to a loss of efficient grain alignment in the cloud, and can result in depolarization in observations. When determining the inclination of the magnetic field on the plane-of-sky, it is assumed that the dispersion of the  $B_{POS}$  small. If uniform grain alignment is assumed, the inclination angle becomes the dominant source of depolarization. This means that even a slight deviation in the magnetic field direction from the line-of-sight (LOS) can cause significant depolarization. So for clouds with a high inclination in magnetic field, there can be a decrease in observed polarization (Chen et al. (2019)).

Grain alignment is also an important factor in the depolarization of light from molecular clouds. This can be directly related to the column density in the clouds. As the column density increases, the alignment efficiency of the dust grains decreases. This can occur due to the increase in the probability of the grains undergoing random thermal motion and colliding with other grains. Therefore, when light passes through regions of high column density, the resulting polarization is reduced (Sullivan et al. (2021)).

Depolarization can also be caused by external sources such as turbulence, galactic magnetic fields (GMF), regions of high star forma-

tion, jet outflows from nearby sources, etc. Turbulence can randomize the magnetic field direction, leading to a larger dispersion.

## 2.5 Observation methods

This section will briefly summarize two methods of observing the inclination angle of magnetic fields, Faraday rotation and dust polarization emission. Faraday rotation is a useful technique in determining the  $B_{LOS}$  of magnetic fields and their strength, and dust polarization emission can determine the inclination angle of the field with respect to the plane-of-sky. A combination of these techniques can contribute to a better understanding of the 3D structure of the magnetic fields in molecular clouds.

### 2.5.1 Faraday rotation

The Faraday effect is when an electromagnetic (EM) wave passes through a magnetic field and it's plane of polarization rotates. The amount of rotation is characterised by

$$\Delta\psi = \lambda^2 (0.812 \int n_e \vec{B} \cdot d\vec{l}) = \lambda^2 RM \quad (1)$$

where  $\Delta\psi$  is the amount of rotation (rad),  $\lambda$  is the wavelength of the EM wave(m),  $n_e$  is the electron volume density of the magnetized region ( $\text{cm}^{-3}$ ),  $\vec{B}$  is the magnetic field strength ( $\mu\text{G}$ ), and  $d\vec{l}$  is the path length (pc) (Tahani et al. (2018)).

Measurements of Faraday rotations in molecular clouds can be made using extinction maps to estimate the electron column densities. This provides information of the magnetic field along the line of sight. Tahani et al. (2018) developed a new technique using Faraday rotation to determine the line of sight magnetic field component in molecular clouds. This was tested on Orion A, Orion B, Perseus and California, which were shown to be consistent with Zeeman observations. This paper will test the efficiency of dust polarization observations in estimating the inclination of the magnetic field of Orion A, and will be compared to the results from Tahani et al. (2022).

### 2.5.2 Dust Polarization observations

Molecular clouds are composed of small, non-spherical dust grains. In the presence of a magnetic field, these grains will align with their long axes perpendicular to the magnetic field lines. As a result, the light observed from the cloud will be linearly polarized. The polarization fraction,  $p$ , can be deduced using Stokes parameters, and the orientation of the magnetic field of the cloud can be determined from  $p$  (Sullivan et al. (2021)).

This method allows for large scale plane of sky observations over a wide range of densities. In the low-density interstellar medium (ISM), the maximum polarization fraction is around  $\sim 0.2$ . However, this fraction typically decreases significantly with increasing gas column density, reaching less than 0.01 in starless cores. This significant decrease can be caused as a result of inefficient grain alignment at high visual extinction ( $A_V$ ) due to a range of column densities and filamentary structures in the cloud(Pattle et al. (2022)).

The following section will summarize the methods used to develop the polarization fraction maps, and how the inclination angle of the fields are calculated.

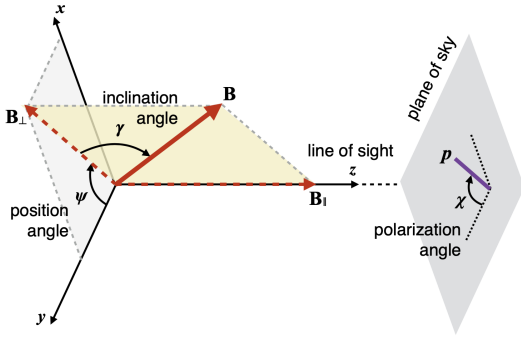


**Figure 1.** Definition of the inclination angle with respect to plane-of-sky component (from Chen et al. (2019))

### 3 METHODS AND TOOLS

Stokes Parameters I, Q, and U are used to determine the polarization fraction of the cloud Sullivan et al. (2021). Using these parameters, the polarization fraction from observations are given by

$$p = \frac{\sqrt{Q^2 + U^2}}{I}. \quad (2)$$

The polarization fraction is determined by the inclination angle,  $\gamma$ , and the dispersion of position angle along the line of sight,  $\psi$ , as shown in figure 1. In the ideal scenario where there is no variation in  $\gamma$  or  $\psi$  along the line of sight, the polarization fraction can be given by

$$p = \frac{p_0 \cos^2 \gamma}{1 - p_0 \left( \cos^2 \gamma - \frac{2}{3} \right)} \text{ (Chen et al. (2019))}. \quad (3)$$

From this equation, the maximum value of  $p$  is when  $\cos^2 \gamma = 1$ , or  $\gamma = 0$ , and the magnetic field is completely on the plane of sky. The maximum observed polarization fraction is thus

$$p_{max} = \frac{p_0}{1 - \frac{1}{3} p_0}, \quad (4)$$

where  $p_0$  represents a polarization coefficient determined by the region of the cloud where  $\gamma$  is the smallest. This variable takes into account the dust grain properties of the cloud, such as the size distribution and alignment efficiency of the grains. Once  $p_0$  is determined from the maximum observed polarization fraction,  $p_{max}$ , this can be used to find  $\gamma_{obs}$ ,

$$p_{obs} = \frac{p_0 \cos^2 \gamma_{obs}}{1 - p_0 \left( \cos^2 \gamma_{obs} - \frac{2}{3} \right)} \quad (5)$$

and rearranging to get,

$$\cos^2 \gamma_{obs} = \frac{p_{obs} \left( 1 + \frac{2}{3} p_0 \right)}{p_0 \left( 1 + p_{obs} \right)}. \quad (6)$$

This result comes from the approximation that there is no variation in  $\gamma$  or  $\psi$  along the line of sight, and that the grain alignment is homogeneous. Thus, this model would be less accurate in a disordered magnetic field. Therefore the error in the derived inclination angle will increase with the perturbation in the cloud. In Chen et al. (2019), this model was tested on Monte Carlo simulations to determine the accuracy of this  $p$ -derived inclination angle.

The dispersion of polarization angles,  $S$ , is calculated at each pixel, and averages the difference between the direction of the polarization vectors at the pixel  $x$  and  $x_i$ , located at a distance  $\delta$

$$S^2(x, \delta) = \frac{\sum \Delta \chi^2(x, x_i)}{\text{number of } x_i} \quad (7)$$

and  $\Delta \chi$ , as shown in figure 1, is

$$\chi = \frac{1}{2} \arctan(u, q) \quad (8)$$

$$\Delta \chi = \frac{1}{2} \arctan2(q(x_i)u(x) - q(x)u(x_i), q(x_i)q(x) + u(x_i)u(x)). \quad (9)$$

where  $\chi$  is the inferred polarization on the plane-of-sky, and  $\Delta \chi$  is the angular difference in polarization between pixels  $x$  and  $x_i$  (Chen et al. (2019)).

Monte Carlo simulations carried out based on these calculations concluded that the smallest values in  $\gamma$  and  $\Psi$  result in the best estimate. It was also concluded that the equation 6 works best when the dispersion angle,  $S$ , is small.

### 4 OBSERVATIONS

This study uses 500  $\mu\text{m}$  polarimetric observations of Vela C molecular cloud from Balloon-borne Large Aperture Submillimeter Telescope for Polarimetry (BLASTPoL) (Fissel et al. (2016)), and 353GHz column density maps of Orion A from the Planck satellite. Vela C is broken up into 5 different regions based on multi-resolution analysis (MRA) of column density and temperature maps by Hill et al. (2011). The inclination angles of four of these regions will be determined: the Center-Ridge, Center-Nest, South-Ridge, and South-Nest (seen in figure 2). Observations of the North, the fifth region in Vela C, were not made by BLASTPoL, and will not be taken into account when measuring the inclination angles. The polarization maps were obtained from Fissel et al. (2016), and created using equation 2. The inclination angles will be determined using the polarization fraction in regions of lower  $S$  dispersion values.

Similarly, Orion A will be broken up into 9 regions based on column density and filamentary structure. We will look at how the polarization fraction changes throughout the cloud, and how this could possibly be affected by the density in different regions of the cloud. To determine if a relationship can be seen between  $p$  and  $N_H$ , 2D histograms will be made to compare the two parameters. These results will be compared to the results from Tahani (2022), to determine if the values can be compared with the measured inclination angle of the magnetic field. In addition, the inclination angle will also be calculated using the polarization fraction, as was done for Vela C. As the  $S$  dispersion is not accounted for in Orion A, these values will be an estimate of the overall inclination angles for each region.

#### 4.1 The Vela C molecular cloud

This study uses 500  $\mu\text{m}$  polarimetric observations of the Vela C molecular cloud, smoothed to a resolution of 2.5' from BLAST-PoL. The maps for the polarization fraction,  $p$ , and the dispersion in polarization angles,  $S$ , were determined from equations 2 and 7 respectively, and obtained from Fissel et al. (2016) (Figure 3). Vela C is a large cloud of  $\sim 30$  pc, with a mass of  $\sim 10^5 M_\odot$ , at a distance of  $700 \pm 200$  pc away and a relatively low temperature of  $\leq 15\text{K}$  (Chen

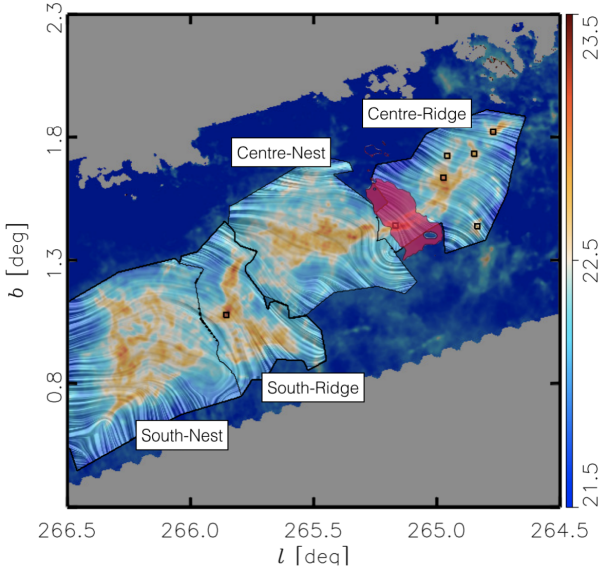


**Figure 2.** Sub-regions and magnetic field lines of the Vela C molecular cloud, as measured by BLASTPol (from Soler et al. (2017)). The field lines indicated by the "drapery" pattern show the field lines projected onto the plane-of-sky. The hydrogen column density filaments can be seen in the center of the cloud, where the colors are given by  $\log(N_H)$ . The squares indicate high mass cores and the region in magenta has a higher temperature due to a massive cluster of stars.

et al. (2019)). Previous polarimetric observations have been made of Vela C to determine its inclination angle and column density properties (Chen et al. (2019); Fissel et al. (2016)). In the following sections, the magnetic field orientation will be determined in each of the regions to determine how its inclination angle can change based on the clouds structure and column density properties.

#### 4.1.1 Subregions and Filamentary Structure

Vela C is broken up into five different subregions based on multi-resolution analysis (MRA) of column density and temperature maps by Hill et al. (2011). The inclination angles of four of these regions will be determined: the Center-Ridge, Center-Nest, South-Ridge, and South-Nest. Polarimetric observations of the North, the fifth region in Vela C, were not made by BLASTPol, and will not be taken into account when measuring the inclination angles. The four regions can be seen in figure 2. The "nests" depict a disorganized network of filaments, whereas the "ridges" have one dominating filament. The regions were determined using an  $A_V = 7$  mag threshold, with cooler, overlapping filaments in the South-Nest region to a more compact, higher density Center-Ridge. The Center-Ridge and South-Nest are the most contrasting regions of the cloud with respect to temperature and column density. The Center-Ridge also appears to be more efficient in star formation than the South-Nest. There is also a small velocity gradient throughout the cloud (Hill et al. (2011)).

By analysing the column density and temperature of these subregions, they can be characterised in their efficiency to form stars in the near future. High mass compact regions ranging from  $20 - 60 M_\odot$  were found in the cloud, corresponding to starless or protostellar dense cores. Among these, six were found in the Center-Ridge, four in the North, two in the Center-Nest, one in the South-Ridge, and none in the South-Nest. Each sub-region contains approximately the same amount of total mass, and is predicted to form approximately

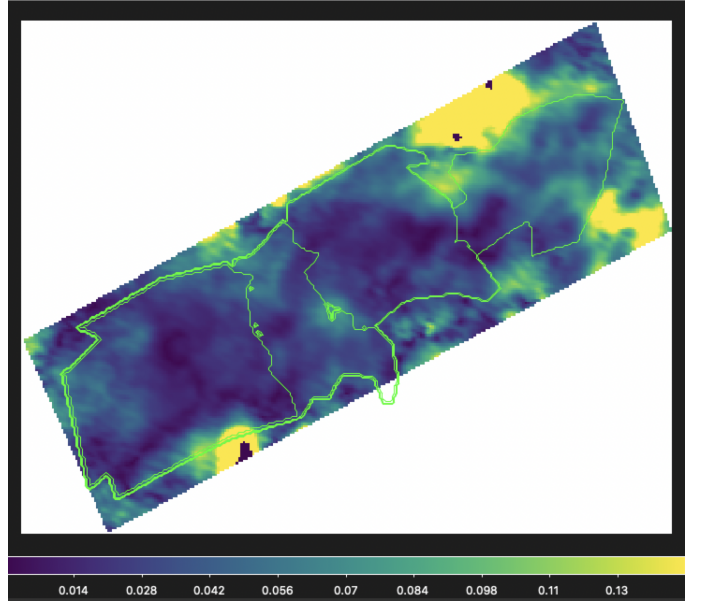


**Figure 3.** Polarization fraction in the Vela C molecular cloud (Fissel et al. (2016)).

the same number of stars. However, since the Center-Ridge contains more massive and denser cores than the South-Nest, it may correspond to the formation of high-mass stars (Hill et al. (2011)).

#### 4.1.2 Results

To determine statistically significant regions of observations, polarization-based cuts were applied to the observed polarization fraction,  $p_{obs}$ . This is to ensure that the values of  $p_{obs}$  were large enough to be unaffected by uncertainties in instrumentation (Fissel et al. (2016)). Regions were masked out using the strength of the polarized intensity,  $P$ , and its uncertainty,  $\sigma_P$ , given by

$$P < 3\sigma_P. \quad (10)$$

To further investigate the magnetic field properties in Vela C, the  $p$ -derived  $\gamma_{obs}$  and the  $S$ -corrected  $\gamma_{obs}$  inclination angles were computed, given in table 1. The  $p$ -derived  $\gamma_{obs}$  refers to the inclination angle derived directly from the polarization fraction  $p_{obs}$ , as given by equation 2. The  $S$ -corrected  $\gamma_{obs}$  takes into account the dispersion in the polarization angle. It has been shown that lower  $S$  dispersion values give a more accurate estimate of the inclination angles in the cloud (Chen et al. (2019)). Thus, from all the polarization fraction values, the  $S$ -derived  $\gamma_{obs}$  values take into account the lower range of the dispersion, which is given by  $S < \langle S \rangle$ . The  $\langle S \rangle$  value is the average of  $S$  taken over the whole cloud. This same  $\langle S \rangle$  threshold cut is applied to each of the individual regions, when determining their inclination angles.

Another important aspect of this analysis was the polarization coefficient,  $p_0$ , which is determined from the maximum polarization fraction,  $p_{max}$  (equation 4). The  $p_0$  value used in this study was found in Chen et al. (2019) to be  $p_0 = 0.15$  across the whole cloud, corresponding to the lowest  $\gamma_{obs}$  value in the cloud. Because this does not necessarily mean that  $\gamma_{obs} = 0$ , the coefficient can be different in different regions of the cloud. In this analysis, the polarization coefficient is assumed to be the same throughout the cloud, and  $p_0 = 0.15$  is used for all four regions.

The overall inclination angle of Vela C using the  $p$ -derived values

was determined to be  $\gamma_{obs} = 66.5^\circ$ , given by the mode of the distribution in figure 4. Calculating the inclination angle using only low- $S$  sightlines, the inclination angle was  $\gamma_{obs} = 55.5^\circ$ , as shown in figure 4. This is in agreement with the results of Chen et al. (2019), where  $\gamma_{obs}$  of the polarized fraction of the overall cloud was determined to be  $64.9^\circ$  and correcting for the  $S$  dispersion, the inclination angle of the magnetic field found was  $54.5^\circ$ .

The values in table 1 give the mode of the inclination angles of the regions, shown as the vertical dashed lines in figure 4 and 5. The  $\gamma_{obs}$  derived by considering the lower limit of the  $S$ -dispersion show that the lowest inclination angle of  $55.5^\circ$  is in the Center-Ridge (figure 5b), whereas the highest inclination angle of  $66.5^\circ$  is in the South-Nest (figure 5c). The overall inclination angle in the South regions are higher in comparison to the Center regions. This gives insight into the 3D structure of the magnetic field, as it shows an increase in the inclination angle of the magnetic field from the Center regions to the South regions.

The filamentary structure of each of the regions in Vela C can be seen in figure 2. The "nests" are made up of multiple smaller filamentary structures, in comparison to the ridges, which have one dominant filamentary structure. The results of the derived inclination angles, in figure 5, show that the Center-Nest and the South-Nest have higher dispersion in polarization fraction compared to the Center-Ridge and South-Ridge. A high dispersion in the polarization fraction indicates that the polarization can vary across the region. This is also seen in the polarization map in figure 3, where the polarization in ridges are lower than they are in the nests. When deriving the inclination after removing values where  $S < \langle S \rangle$ , there are significantly fewer values in the nests, when compared to the ridges, seen in figure 5. The Center-Nest and the South-Nest appear to have the highest amount of dispersion (figures 5a and 5c), and the Center Ridge and South Ridge have lower dispersion in comparison (figures 5b and 5d). This can correspond to either a weak magnetic field, or a significant fraction of the inclination angle of the field in the line of sight direction. The variation in polarization fraction can also be due to low grain alignment efficiency in the cloud due to factors such as the column density and grain alignment efficiency.

#### 4.1.3 Discussion

Chen et al. (2019) developed a new method to determine the inclination angle of the magnetic fields in molecular clouds using the dust polarization. By considering regions of low  $S$  dispersion, the synthetic observations gave estimates of the orientation of inclination angle to within  $\lesssim 10^\circ - 30^\circ$ . Using these results, Vela C was determined to have an overall high inclination angle of  $60^\circ - 65^\circ$  with respect to the plane of sky. Additionally, Chen et al. (2019) proposed that changes in the polarization observed in the cloud are primarily caused by changes in the magnetic field configuration rather than differences in the efficiency of grain alignment. Thus from the observations in each of these regions, it can be seen that Vela C has a high inclination angle, that increases toward the south regions of the cloud.

Based on the high inclination of the cloud, a significant source of depolarization in Vela C can result from the inclination angle. The  $S$ -dispersion value is assumed to be the same in the cloud, although the inclination angle is shown to be higher in the south. If the  $S$ -dispersion were to be taken individually in each of the regions, a better estimate of the inclination angle can be calculated in regions where the angle is closer to the plane-of-sky.

Additionally, a  $p_0$  value of 0.15 was assumed throughout the cloud. As this is derived from the lowest possible inclination in the region,

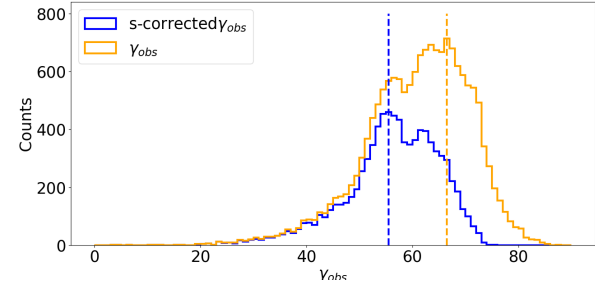


**Figure 4.** Inclination angle over the whole Vela C cloud. The most probable  $\gamma_{obs}$  value is  $66.5^\circ$ . Correcting for the  $S$  dispersion, the most probable  $\gamma_{obs}$  value is  $55.5^\circ$ , in agreement with observations from Chen et al. (2019) and Sullivan et al. (2021).

	<i>p</i> derived $\gamma_{obs}$	<i>S</i> corrected $\gamma_{obs}$
Whole Cloud	$66.5^\circ$	$55.5^\circ$
Center-Ridge	$55.5^\circ$	$54.5^\circ$
Center-Nest	$67.5^\circ$	$54.5^\circ$
South-Ridge	$61.5^\circ$	$61.5^\circ$
South-Nest	$66.5^\circ$	$66.5^\circ$

**Table 1.**  $\gamma_{obs}$  values derived for the Vela C molecular cloud.  $\gamma_{obs}$  gives most probable inclination angle. The  $S$ -corrected  $\gamma_{obs}$  values were determined using points in the cloud where  $S < \langle S \rangle$ .

the value can differ in different regions. Measuring the  $p_0$  for the individual regions can also be considered in improving the accuracy of the calculated angles.

Fissel et al. (2016) reported a clear anti-correlation between the column density  $N_H$  and  $p$  in Vela C. This correlation has also been observed in studies of other clouds using similar methods (Sullivan et al. (2021); King et al. (2017)). The decrease in polarization for increase in  $N$  can also be due to a cancellation in sightlines due to a disorder in the magnetic field. While this does not significantly affect Vela C as determined by synthetic observations in Chen et al. (2019), it could affect observations of other molecular clouds based on their structures.

## 4.2 The Orion A molecular cloud

This study uses 353GHz polarimetric observations of the Orion A molecular cloud, with a resolution of  $15'$ , from the *Planck* Satellite. It spans a distance of 391 to 445 pc, with a median distance of 405 pc (Zucker et al. (2021)). The study of the Orion A molecular cloud involved an analysis of its polarization fraction and the column density, and 2D histograms of these parameters were created. Previous observations by Tahani (2022) show that the magnetic field is changing throughout the cloud, and is described to have an arc-shaped morphology. The polarization of Orion A will be analysed to determine if it aligns with the Faraday rotation observations.

### 4.2.1 Subregions and Substructures

Orion A was divided into 9 different regions, as shown in figure 8. It is broken up into 4 main regions, A-D, that span horizontally

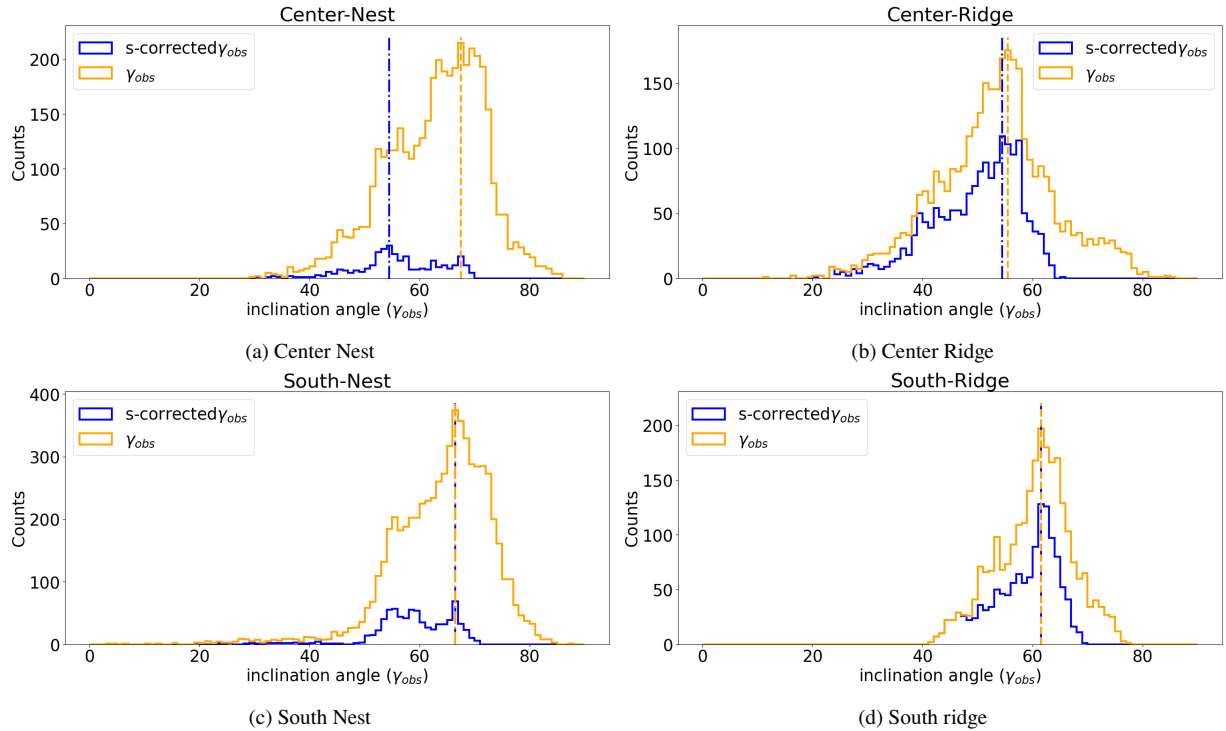


**Figure 5.** These figures show the  $p$  derived inclination angles in comparison with the  $\mathcal{S}$ -corrected inclination angles for each of the subregions in Vela C. The dispersion of the polarization angles,  $\mathcal{S}$ , as well as factors in different regions of the cloud can affect the perceived inclination angle of the magnetic field. The vertical lines show the mode of the inclination angles corresponding to the most probable value of the inclination angle in the given region of the cloud.

across the cloud and each of these regions are divided based on its column density and magnetic field properties. In the regions labeled '1', Tahani (2022) found that the magnetic field in these regions point towards us, whereas in regions labeled '3', the field points away from us, as shown in figure 6, which shows a reversal in the line of sight of the magnetic field,  $B_{LOS}$ , throughout the cloud. Regions labeled '2' runs along the filament, and contains regions of higher column density. We will analyse the polarization fraction in each of these regions to determine how it compares with the structure of the cloud and its magnetic field.

#### 4.2.2 Results

The polarization of Orion A was analysed in three parts. The first part was graphing the polarization fraction as a function of the position in the cloud, to see how it changes throughout the cloud. The second part looks at the relationship between the column density and the polarization using 2D histograms. Finally, the overall inclination angle,  $\gamma_{obs}$ , will be measured to gain a better understanding of the 3D structure of the cloud's magnetic field.

The change in polarization fraction throughout the cloud is shown in figure 7, for six regions of the cloud. For each region, we plot the median polarization fraction (x-axis) as a function of vertical position. In examining the polarization fraction, an increase can be seen right above the filament in the cloud. There is a dip in the polarization fraction, and a slight increase in the polarization fraction below the filament. This dip in the polarization can be further analysed by considering how the structure of the cloud changes in high column density regions, and can be attributed to the lower grain alignment efficiency in that region.

2D histograms of the polarization fraction and column density for

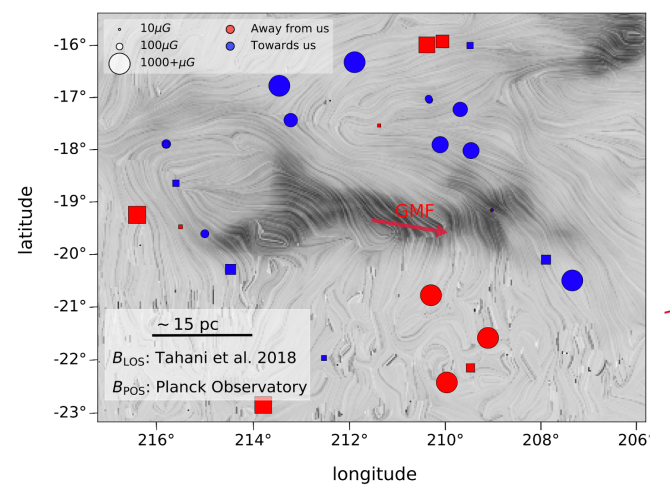


**Figure 6.** The structure of the magnetic field of the Orion A molecular cloud, as shown in Tahani (2022). The filamentary structure illustrates the hydrogen column density of the cloud. The blue and red markers represent the  $B_{LOS}$  towards and away from us, respectively. The squares indicate non-detection points (with high uncertainties that may cause a change in  $B_{LOS}$  direction). The size of the markers represent the strength of the field. The drapery lines represent the  $B_{POS}$  observed by the Planck Space Observatory. The red 'GMF' vector shows the Galactic Magnetic Field (GMF) projected on the plane-of-sky (Tahani (2022)).

these regions are shown in figure 9, where the white dotted lines show the median of the polarization fraction for a change in the column density. We can see that in regions of high column density, B2, C2, and D2, the polarization fraction is typically low. In D2

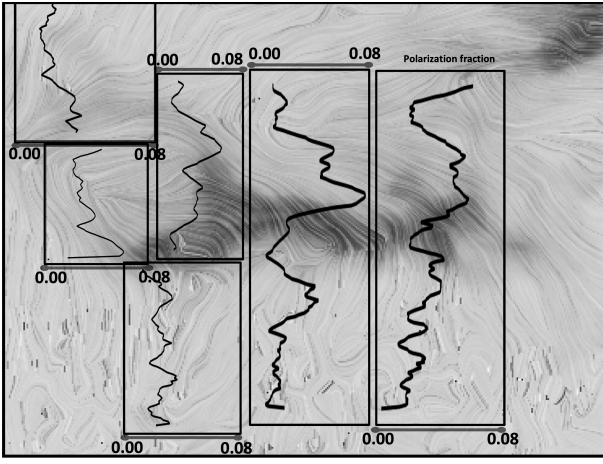


**Figure 7.** The change in the polarization fraction throughout the cloud, illustrated on a hydrogen column density map of Orion A (Tahani (2022)), overlaid on the same column density map as in figure 6. The filament can be seen by the dark region in the center, where there is an increase in the polarization fraction immediately above the filament. The polarization fraction range for each region is 0.00 to 0.08.

(fig. 9h), there is an increase in the polarization fraction towards lower column densities in the cloud, and we can see a decrease in  $p$  as  $N_H$  increases, which aligns with the negative correlation from previous studies Planck Collaboration XIX (2015); Sullivan et al. (2021). We also see higher polarization fractions in regions A1, B1 and C1, which are regions of lower column density above the cloud. As mentioned previously, these can correspond with the increase in the polarization fraction seen above the filament in figure 7.

The decrease in polarization fraction in the filament can be due to its high column density. As the polarization fraction relies on the alignment of grains with the magnetic field in the cloud, a decrease in the polarization fraction is likely due to the decreased grain alignment in regions of higher column density. Dust grains in high density regions can be affected by various factors leading to random orientations that reduce the degree of alignment necessary for producing high polarization fractions. In regions of lower column density, dust grains may have more freedom to align with the magnetic field, resulting in a higher polarization fraction.

The inclination angle in these regions can be measured from the polarization fraction, using the same method used for the Vela C molecular cloud. For Orion A, the  $S$  dispersion is not taken into account, so this method will give a rough estimate of the overall orientation of the magnetic field in the cloud. In the results in Vela C, the  $p$  derived inclination was usually close to the  $S$  corrected inclination angle of the magnetic field. While this can vary across different clouds due to variations in grain alignment and column density, the inclination angle determined by  $p$  can give an estimate of the overall orientation of the magnetic field in the cloud. The inclination angle of each of the regions is given in table 2, and there is an overall high inclination angle ranging from  $50^\circ$  to  $66^\circ$  in the cloud, similar to Vela C. For regions '1' and '3', this aligns with from Tahani (2022) in figure 6, where the magnetic field in those regions point towards and away from us, respectively. Results from region '2' along the filament are uncertain due to the lower polarization properties, possibly from the column density and grain alignment in these regions. This could give an artificially high estimate of the inclination angle.

It should be noted that the polarization coefficient used for this

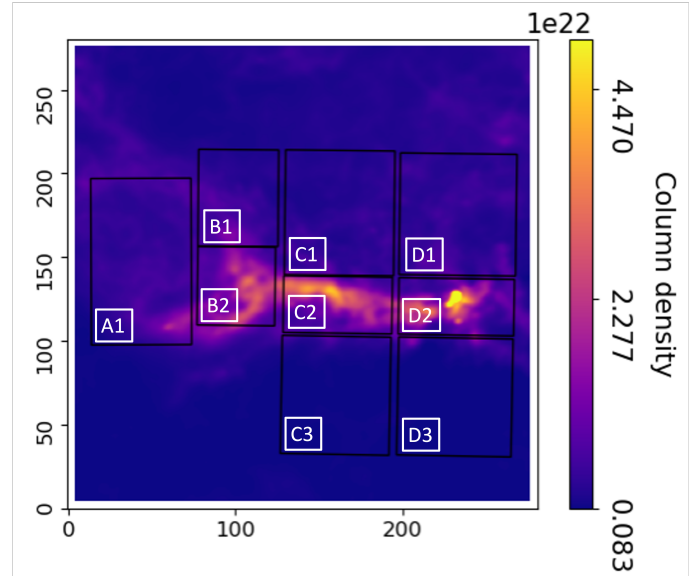


**Figure 8.** Column density plot of Orion A. Regions are broken up based on filamentary structure to analyse how the polarization fraction changes throughout the cloud. 2D histograms of each region is plotted for  $p$  vs  $N_H$  in figure 9.

cloud is the same as in Vela C, at  $p = 0.15$ , although this value is likely to differ for different clouds. For more thorough measurements of the inclination angle, a more accurate value of the polarization coefficient should be considered. Since observations from Tahani (2022) indicate that the inclination angles are higher around the filament, the polarization coefficient will likely also change in these regions, and must be considered.

#### 4.2.3 Discussion

From figure 6, Tahani (2022) concluded that based on the reversal in the field, the structure of the field most likely has an arc-shaped morphology. Thus the orientation of the field around the cloud would be higher, and is likely to be close to  $\gamma = 0$  towards the center of the cloud. This would imply a high polarization fraction at the filament in comparison to the regions around the filament. However, as seen in figure 7, there was observed to be a dip in the polarization fraction at the filament. This can likely correspond with the relationship between the  $p$  and  $N_H$ . As there is an increasing column density at the filament (figure 9), this can suggest a lower grain alignment from those regions.

The negative correlation observed between column density and polarization fraction suggests that it is easier to deduce the polarization fraction in regions of lower column density than in regions of higher column density. This correlation also agrees with similar observations by Sullivan et al. (2021), where 6 out of 9 surveyed clouds showed a decrease in  $p$  for an increase in  $N_H$ .

For regions around the filament, an overall high inclination angle is measured, with values of  $50^\circ$ – $66^\circ$  (Table 2). Due to the low polarization at the center of the cloud, the values may not correspond to the actual inclination angles in the cloud, and further analysis would be required to account for the column density properties of the cloud. However, the column density around the filament is lower, and there is an increase in the polarization fraction. This can indicate a magnetic field inclination that is closer to the plane-of-sky.

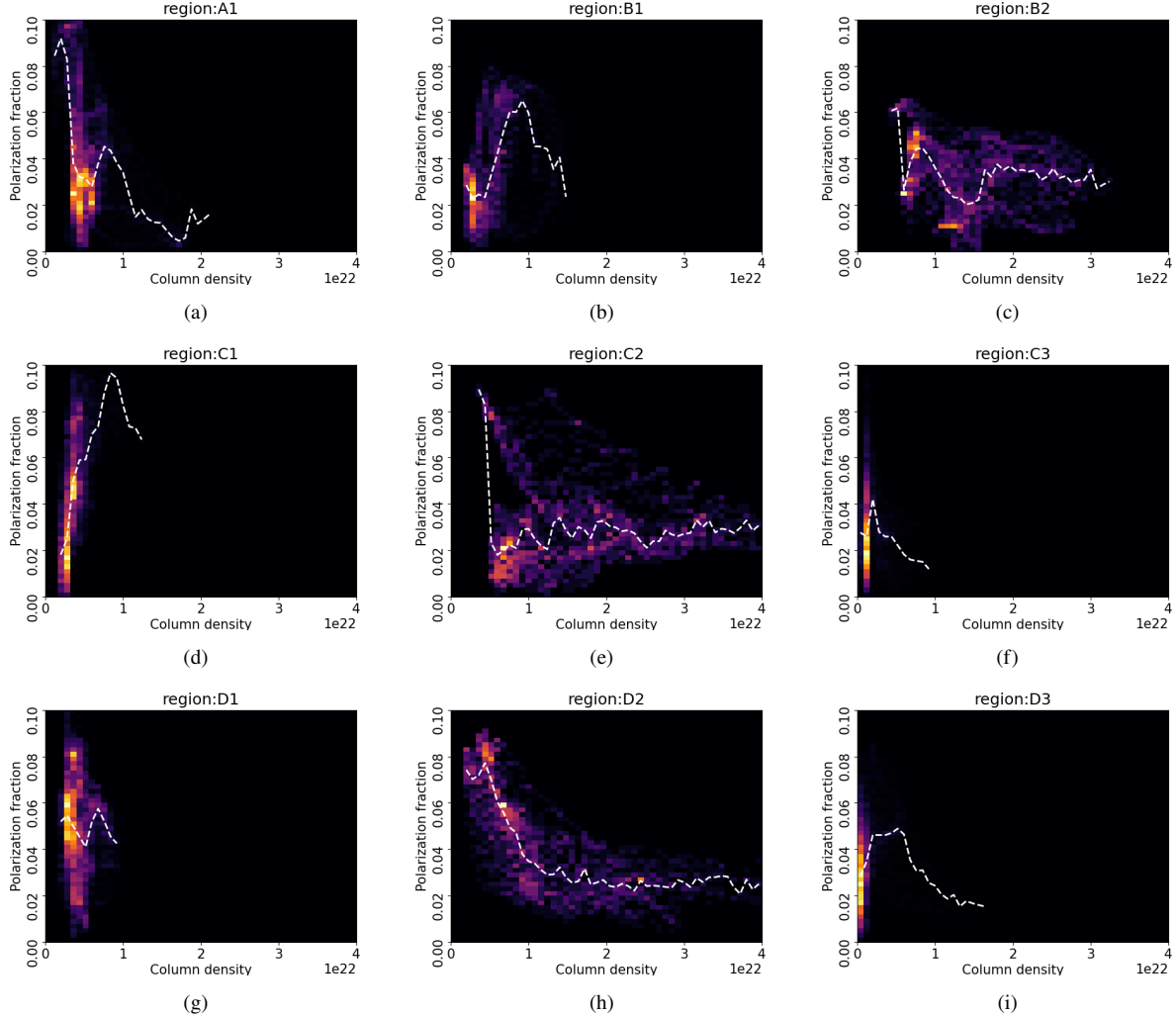


**Figure 9.** 2D histograms of the polarization fraction plotted against column density of Orion A. Each region corresponds to the column density map in figure 8. The dotted lines represent the median of the polarization for the given range of column densities.

	$\gamma_{obs}$	$\gamma_{obs}$	$\gamma_{obs}$	$\gamma_{obs}$	
<b>A1</b>	63°	<b>B1</b>	50°	<b>C1</b>	66°
		<b>B2</b>	62°	<b>C2</b>	53°
			<b>D1</b>	59°	
			<b>D2</b>	62°	
			<b>C3</b>	64°	
			<b>D3</b>	61°	

**Table 2.**  $p$  derived inclination angles of the Orion A regions

## 5 SUMMARY

The goal of this study was to analyze the 3D magnetic field properties of molecular clouds using dust polarization observations. The Vela C and Orion A molecular clouds were analyzed based on their polarimetric observations. In Vela C, the inclination angle was determined based on the polarization fraction and the dispersion of position angle along the line of sight. It was found that Vela C has a high overall inclination angle, which was determined based on synthetic observations from previous studies in Chen et al. (2019). The cloud was divided into four regions based on column density and temperature variations, and the inclination angle was computed

for each region, revealing that it increases towards the south of the cloud. In particular, the dispersion in polarization fraction was found to be significantly higher in the Center-Nest and South-Nest regions where there were multiple overlapping structures, compared to the Center-Ridge and the South-Ridge, where there was a dominant filamentary structure. This suggests that the filamentary structure and column density are factors that can affect the dispersion in polarization angle. The mode of the inclination angles also differed between the regions, with higher angles in the south and lower angles in the center, indicating an increase in the orientation of the magnetic field. The polarization coefficient,  $p_0$ , was assumed to be constant throughout the cloud, but it can differ in different regions, which future studies should take into account. Similarly, the  $\langle S \rangle$  was taken over the whole cloud, and was applied to all regions to eliminate areas of high dispersion. As the dispersion can differ in various regions of the cloud, another approach to this can involve applying the  $\langle S \rangle$  value of individual regions to eliminate areas of high dispersion.

In Orion A, the polarization was observed in various regions, to determine how it can change as a result of the column density. The cloud was divided into 9 regions based on its column density. It was found that there was a dip in the polarization fraction at the center of the cloud, which could be attributed to higher column density and

lower grain alignment efficiency. Additionally, there was a reversal in the magnetic field around the cloud, as reported by Tahani, was not entirely reflected by the polarization fraction. Above the main filamentary structure, there was an increase in the polarization fraction, as well as a slight increase right below the filament. This was attributed to more efficient grain alignment in low column density regions. The increase in the polarization fraction could also indicate that the orientation of the magnetic field is closer to the plane-of-sky. 2D histograms showed that regions of high column density had a lower median polarization fraction, while regions of lower column density had a higher median polarization fraction. Additionally, Orion A was found to have an overall high inclination, with values from  $50^\circ - 66^\circ$ , which aligns with the high inclination angles around the cloud, as determined by [Tahani et al. \(2018\)](#).

The analysis of polarization properties in Vela C and Orion A has provided valuable insights into the 3D structure of the cloud's magnetic field and its relationship with column density. However, there are many factors still to be taken into consideration, such as determining the polarization coefficient,  $p_0$  in different regions of the cloud, as this can vary based on individual cloud structures. The dispersion in  $\mathcal{S}$  can also vary based on different inclination angles in the cloud, as was seen in Vela C, and can be improved by analysing the  $\langle \mathcal{S} \rangle$  value for each region individually. In order to further our understanding of the role of magnetic fields in star formation, future studies should take into account these factors and continue to analyze polarization properties in molecular clouds. For example, breaking down clouds into sub-regions, as was done for Vela C in parts of this study, can provide more detailed insights into the magnetic field morphology of these regions. Additionally, it is important to consider observational biases that may affect polarization measurements, such as sightline selection criteria and background and foreground emission. By taking these factors into account, we can continue to improve our understanding of the complex relationship between magnetic fields and star formation in molecular clouds.

## REFERENCES

- Aghanim N., et al., 2020, *Astronomy & Astrophysics*, 641, A12
- Chen C.-Y., King P. K., Li Z.-Y., Fissel L. M., Mazzei R. R., 2019, *Monthly Notices of the Royal Astronomical Society*, 485, 3499
- Fissel L. M., et al., 2016, *The Astrophysical Journal*, 824, 134
- Hill T., et al., 2011, *Astronomy & Astrophysics*, 533, A94
- King P. K., Fissel L. M., Chen C.-Y., Li Z.-Y., 2017, *Monthly Notices of the Royal Astronomical Society*, 474, 5122
- Pattle K., Fissel L., Tahani M., Liu T., Ntormousi E., 2022, Magnetic fields in star formation: from clouds to cores, doi:10.48550/ARXIV.2203.11179, <https://arxiv.org/abs/2203.11179>
- Planck Collaboration XIX e. a., 2015, *Astronomy & Astrophysics*, 576, A104
- Soler J. D., et al., 2017, *Astronomy & Astrophysics*, 603, A64
- Sullivan C. H., Fissel L. M., King P. K., Chen C.-Y., Li Z.-Y., Soler J. D., 2021, *Monthly Notices of the Royal Astronomical Society*, 503, 5006
- Tahani M., 2022, *Frontiers in Astronomy and Space Sciences*, 9
- Tahani M., Plume R., Brown J. C., Kainulainen J., 2018, *Astronomy & Astrophysics*, 614, A100
- Tahani M., et al., 2022, *Astronomy & Astrophysics*, 660, A97
- Zucker C., et al., 2021, *The Astrophysical Journal*

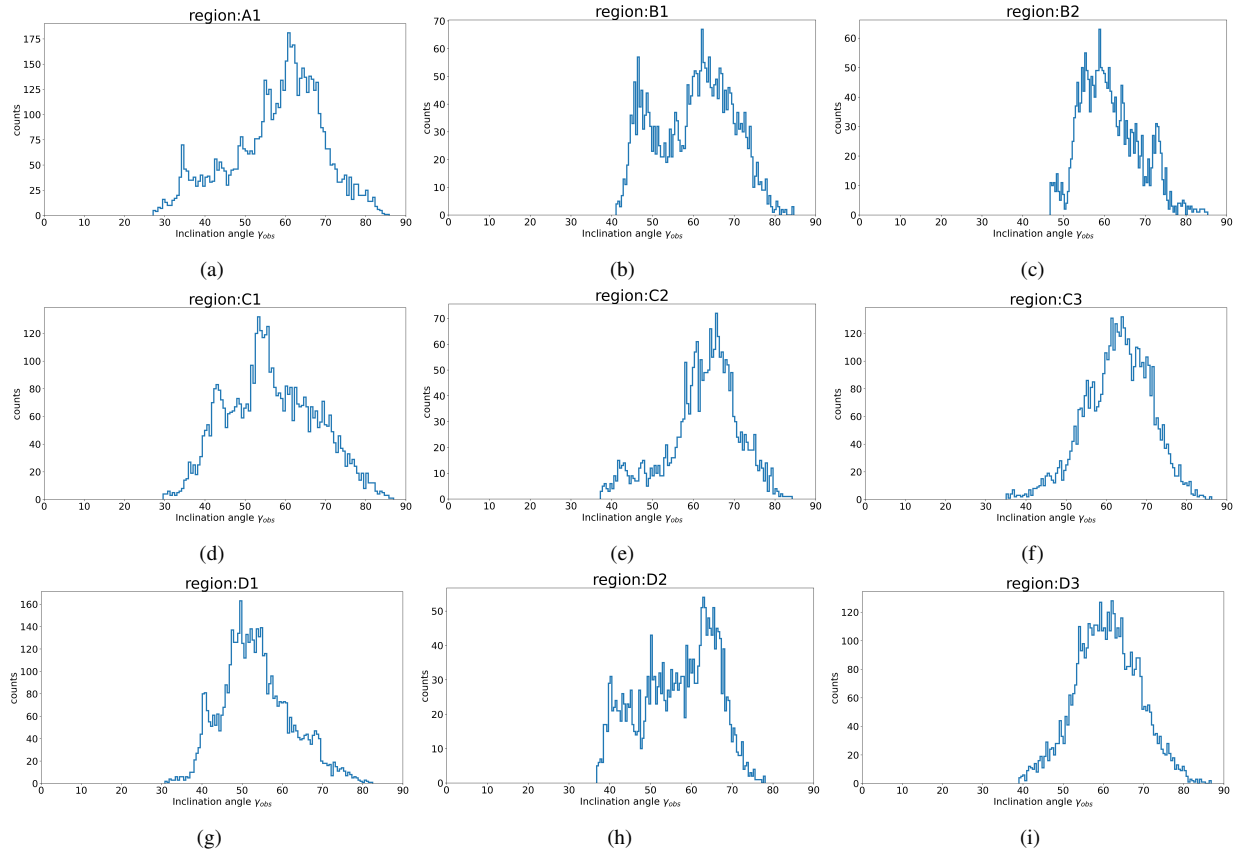


**Figure 10.** Inclination angles of regions in Orion A.